JOC*Note*

Stereomutation of Conformational Enantiomers of 9-Isopropyl-9-formylfluorene and Related Acyl Derivatives

Daniele Casarini,*[,†] Lodovico Lunazzi,[‡] and Andrea Mazzanti*[,‡]

Department of Chemistry, University of Basilicata, via N. Sauro 85, Potenza 85100, Italy, and Department of Organic Chemistry "A. Mangini", University of Bologna, Viale Risorgimento 4, Bologna 40136, Italy

casarini@unibas.it; mazzand@ms.fci.unibo.it

Received April 24, 2008

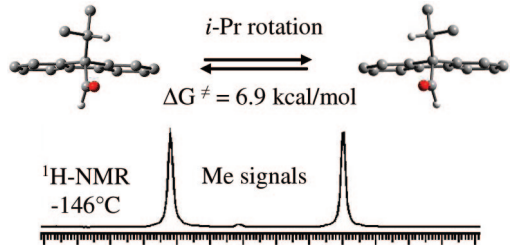

Low-temperature NMR spectra show that the title compound exists as a pair of conformational enantiomers, generated by the restricted rotation about the C9−Pr^i bond, the corresponding interconversion barrier being 6.9 kcal mol^{-1}. This interpretation is supported by theoretical (MM and DFT) calculations and by the experimental determination of the analogous barriers occurring in the related MeC═O and Bu^{t}C═O derivatives.

Restricted rotation processes have been observed in a variety of fluorenyl derivatives bearing at least one aryl substituent in position 9.[1,2] The large number of reported examples is due to the fact that the corresponding barriers are relatively high, thus quite easy to detecte by NMR technique. On the other hand, the barriers for the analogous processes occurring in the alkylfluorenyl derivatives are expected to be very low, thus accounting for the absence of these values in the literature (only very recently has one such case been detected[3]). We report here a study of the dynamics of the rotation process about the C9−isopropyl bond in the title compound **1** (Chart 1), which has been selected since it is a key intermediate for the preparation of drugs acting as calcium antagonists in the case of cardiovascular activity.[4]

CHART 1

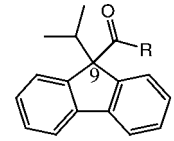

R = H, **1**
= Me, **2**
= Bu^t, **3**

As shown in Figure 1, the ^{13}C methyl signal of **1** broadens on cooling and eventually splits, at −146 °C, into two lines separated by 3.34 ppm. The rate constants derived from line shape simulation yield a free energy of activation of 6.9 kcal mol^{-1} for the observed dynamic process.[5]

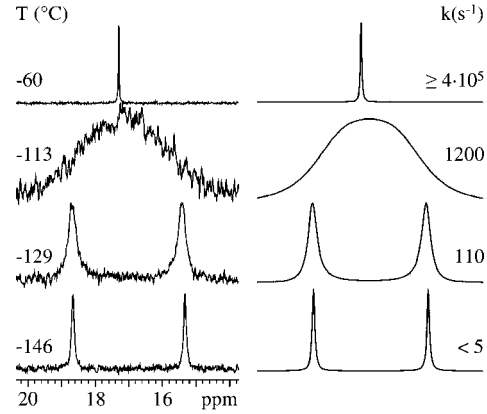

FIGURE 1. Temperature dependence of the ^{13}C methyl signal (150.8 MHz) of **1** in $CHF_2Cl/CHFCl_2$ (left). On the right is displayed the simulation obtained with the rate constants reported.

Also the ^{13}C aromatic signals display the same type of dynamic behavior on lowering the temperature. In Figure 2, for instance, the two lines of the two quaternary carbons broaden and, likewise, split into two pairs of lines at −146 °C.

The barrier derived from this spectrum (6.9 kcal mol^{-1}) is the same as that obtained by the analysis of the methyl signals, thus indicating that both spectra are monitoring the same dynamic process. Analogous spectral features were observed by means of the ^{1}H spectra, as reported in Figures S-1 and S-2 of the Supporting Information.

These results indicate that the molecule adopts an asymmetric conformation (C_1 point group) having lost the dynamic symmetry (C_s) that accounts for the ambient temperature NMR spectrum.

The measured barrier could arise, in principle, from three possible situations: (i) if the C9−CHO rotation is faster than the C9−Pr^i bond rotation, then the latter motion would be responsible for the value of the barrier; (ii) if, on the contrary, the C9−Pr^i bond rotation is the faster of the two motions, the measured barrier would be that due to the rotation about the

[†] University of Basilicata.
[‡] University of Bologna.

(1) See: Oki, M. *Applications of Dynamic NMR Spectroscopy to Organic Chemistry*; VCH Publisher: Deerfield Beach, FL, 1985211
(2) Nishida, A.; Akagawa, Y.; Shirakawa, S.; Fujisaki, S.; Kajigaeshi, S. *Can. J. Chem.* **1991**, *69*, 615–619.
(3) Casarini, D.; Lunazzi, L.; Mazzanti, A. *J. Org. Chem.* **2008**, *73*, 2811–2818.
(4) Gualtieri, F.; Teodori, E.; Bellucci, C.; Pesce, E.; Piacenza, G. *J. Med. Chem.* **1985**, *28*, 1621–1628.
(5) As often observed in conformational processes, the free energy of activation was found independent of temperature within the errors, indicating a negligible value of $\Delta S^{\neq}$. See, for instance: (a) Lunazzi, L.; Mancinelli, M.; Mazzanti, A. *J. Org. Chem.* **2007**, *72*, 5391–5394, and references quoted therein.

10.1021/jo8008897 CCC: $40.75 © 2008 American Chemical Society
Published on Web 07/22/2008

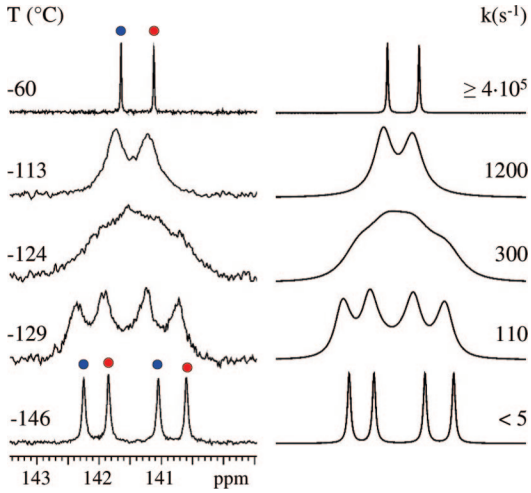

FIGURE 2. Temperature dependence of the ^{13}C signals (150.8 MHz) of the two aromatic quaternary carbons of **1** in $CHF_2Cl/CHFCl_2$ (left). On the right is displayed the simulation obtained with the rate constants reported.

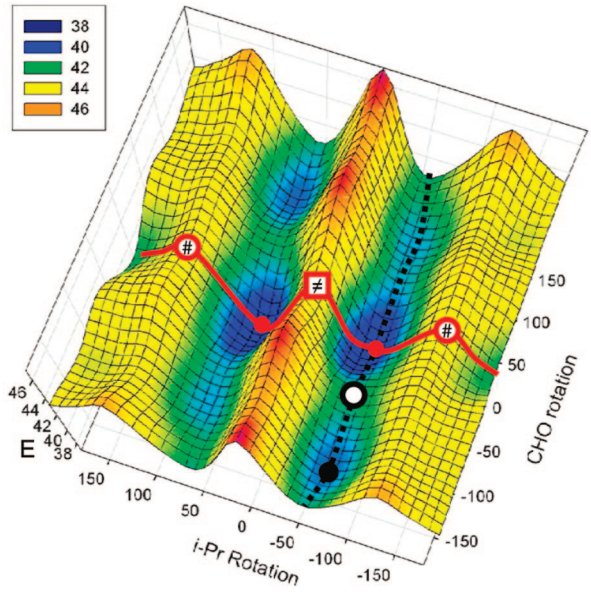

FIGURE 3. MMX computed energy (E in kcal mol^{-1}) surface of **1** as a function of the rotation pathways about the C9−Pr^i (showing the two mentioned transition states) and the C9−CHO bonds (red line and black dotted line, respectively).

C9−CHO bond;[6] and (iii) it is also possible that the two rotations are not independent and, as a result of a correlated process, the measured barrier would be that due to the two motions occurring simultaneously.

To identify the geometries of the energy minima and of the transition states, the three-dimensional energy surface of **1** was computed (MMX force field[7]) as a function of the dihedral angles corresponding to the rotations of the isopropyl and of the HCO substituents (Figure 3).

Three energy minima (indicated by the full dots) were localized on the map: two of them (red dots) correspond to a pair of enantiomers due to the rotation of the isopropyl group,

(6) Even in the hypothesis of a C9−Pr^i faster than the C9−CHO rotation, the two methyl groups will be diastereotopic at −146 °C, owing to the molecular asymmetry (C_1 point group, as in Scheme 1) due to the frozen C9−CHO rotation at that temperature.

(7) MMX force field, PC Model 7.5; Serena Software: Bloomington, IN.

SCHEME 1. The Bottom Part Shows the DFT Computed Enantiomeric Ground State (GS) of 1 and the Top Part the two Possible Transition States (TS-1 and TS-2) for the C9−Pr^i Rotation[a]

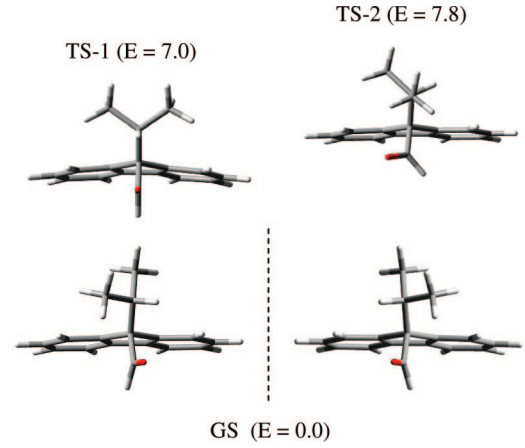

[a] The energies (E) are given in kcal mol^{-1}.

in which the two dihedral angles H−CMe$_2$−C9−CHO and O−C−C9−CHMe$_2$ are 54° and −14°, respectively (see also Scheme 1).[8] The third minimum (black dot) corresponds to a diastereomeric structure due to the C9−CHO rotation, in which the same dihedral angles are 59° and −114°, respectively. This structure, however, is calculated to have an energy higher by 1.3 kcal mol^{-1}.

There are two transition states for the C9−Pr^i bond rotation (indicated by ≠ and # on the red line), the corresponding energies being 5.6 and 7.1 kcal mol^{-1}, respectively. The allowed pathway followed by the C9−Pr^i bond rotation will be, therefore, that involving the lowest of the two barriers (5.6 kcal mol^{-1}). The transition state for the C9−CHO rotation pathway (hollow circle on the black dotted line) has an energy 2.7 kcal mol^{-1} higher than that of the ground state, and corresponds to a dihedral angle O−C−C9−CHMe$_2$ of −54°.

The red and black lines run parallel to the axes, thus indicating that the two motions are independent,[9] so that hypothesis iii of a correlated motion can be discounted. According to these computations, the barrier for the C9−CHO rotation is much lower than that for the C9−Pr^i rotation, and would exchange two diastereomeric conformers of different energy. Furthermore, the predicted barrier for the C9−CHO rotation is too low to be detected in the variable-temperature NMR experiment. These considerations exclude hypothesis ii, indicating that the measured value of 6.9 kcal mol^{-1} corresponds to the C9−Pr^i rotation, i.e., to hypothesis i.

Although the lower MMX computed barrier of 5.6 kcal mol^{-1} is in reasonable agreement with the experiment, it is somewhat inconsistent that the higher (rather than the lower) computed barrier is in better agreement with the measured value. For this

(8) The small angle of 14° suggests, however, that the libration about the plane defined by the dihedral O−C−C9−CHMe$_2$ = 0 might still take place. If the C9−Pr^i bond rotation is fast, this process would create a dynamic plane of symmetry that would render isochronous the isopropyl methyls and aromatic signals, in contrast with the experimental observations at −146 °C.

(9) (a) Grilli, S.; Lunazzi, L.; Mazzanti, A. *J. Org. Chem.* **2001**, *66*, 4444–4446. (b) Grilli, S.; Lunazzi, L.; Mazzanti, A. *J. Org. Chem.* **2001**, *66*, 5853–5858. (c) Jog, P. V.; Brown, R. E.; Bates, D. K. *J. Org. Chem.* **2003**, *68*, 8240–8243. (d) Casarini, D.; Grilli, S.; Lunazzi, L.; Mazzanti, A. *J. Org. Chem.* **2004**, *69*, 345–351. (e) Casarini, D.; Lunazzi, L.; Mazzanti, A.; Mercandelli, P.; Sironi, A. *J. Org. Chem.* **2004**, *69*, 3574–3577. (f) Lunazzi, L.; Mazzanti, A.; Minzoni, M. *Tetrahedron* **2005**, *61*, 6782–6790.

TABLE 1. Experimental and DFT Computed Barriers (kcal mol^{-1}) for the C9−Pr^i Bond Rotation

compd	1	2	3
exptl	6.9	7.9	8.2
DFT computed	7.0	7.8	8.0

reason we recalculated all the stationary points by making use of the more reliable DFT approach.[10]

Indeed DFT calculations confirm that compound **1** does not exhibit any element of symmetry in its ground state and thus exists as a pair of conformational enantiomers (Scheme 1, bottom). The less stable diastereomeric conformer, due to the C9−CHO rotation mentioned above, is calculated to have an energy 1.8 kcal mol^{-1} higher than the ground state (see the Supporting Information), thus it is not appreciably populated.

The two transition states involved in the isopropyl rotation are predicted to be 7.8 and 7.0 kcal mol^{-1} (TS-2 and TS-1, respectively in Scheme 1) higher than the ground state (GS in Scheme 1).[11]The 7.0 kcal mol^{-1} value, being the lower, corresponds therefore to the rotation barrier that the isopropyl group must overcome to interconvert the conformational enantiomers. It is gratifying to observe that the lower DFT barrier is actually the one closer to the experimental value and, in addition, that the agreement with the latter (Table 1) is even better than that obtained by MMX. The DFT computations also confirm that the C9−CHO bond rotation barrier (3.0 kcal mol^{-1}) is too low to be NMR detectable.

To provide experimental support to this interpretation, the dynamic process was investigated also in the case of derivatives **2** (R = Me) and **3** (R = Bu^t).

The ground state conformations calculated for these compounds are similar to that of **1**: the computed prediction of these conformers are quite reliable, as shown in the case of **3** where the X-ray structure was found essentially equal to the computed one (Figure 4).[12]

The temperature dependence of the ^{1}H isopropyl methyl signal[13]of **2** (Figure S-3 of the Supporting Information) yields a barrier of 7.9 kcal mol^{-1} and the ^{13}C isopropyl methyl signal[13]of **3** (Figure S-4 of the Supporting Information) yields a barrier of 8.2 kcal mol^{-1} (Table 1).

The fact that these two barriers are essentially equal within the errors (±0.15 kcal mol^{-1})[14]rules out the possibility that these values correspond to the C9−CO bond rotation: if this was the case, in fact, these values would have been quite different.[15]On the contrary, not only are these barriers are equal, but they are higher than that of aldehyde **1** only by a relatively small amount. This means that the greater dimensions of the MeC═O and Bu^{t}C═O moieties with respect to HC═O produce only a moderate increase of the barrier of the C9−Pr^i bond rotation.[16]

This can be rationalized by considering that it is the C═O moiety that is close to the isopropyl group, whereas the Me and Bu^t groups are far away from it (see, for instance, Figure 4).[17]For this reason their steric effects upon the C9−Pr^i bond rotation are, conceivably, not much larger than that due to HC═O: the difference with respect to the barrier measured in **1** is, in fact, only 1.0 and 1.3 kcal mol^{-1} for **2** and **3**, respectively (Table 1).

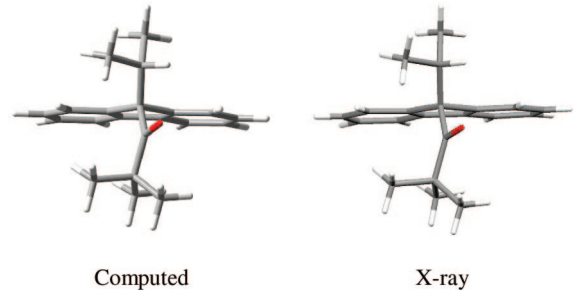

FIGURE 4. DFT computed (left) and X-ray diffraction structure (right) of compound **3**.

Experimental Section

9-Isopropyl-9*H*-fluorene-9-carbaldehyde (1).[4] See the Supporting Information for the detailed synthetic procedure. ^{1}H NMR (600 MHz, CD_3CN, +25 °C) δ 0.78 (d, J = 6.8 Hz, 6H), 2.98 (septet, J = 6.8 Hz, 1H), 7.41 (td, J = 7.5, 1.2 Hz, 2H), 7.49 (td, J = 7.6, 1.1 Hz, 2H), 7.59 (td, J = 7.5, 1.1 Hz, 2H), 7.87 (dt, J = 7.5, 1.1 Hz, 2H), 9.52 (s, CHO). ^{13}C NMR (150.8 MHz, CD_3CN, +25 °C) δ 18.5 (CH_3), 33.9 (CH), 72.6 (C_q), 121.6 (CH), 127.1 (CH), 128.9 (CH), 129.9 (CH), 143.4 (C_q), 143.5 (C_q), 200.7 (CHO). MS m/z (%) 236 ($M^{\bullet+}$, 27), 208 (83), 207 (88), 192 (86), 181 (26), 191 (72), 166 (71), 165 (100). HRMS calcd for $C_{17}H_{16}O$ 236.12012, found 236.1200.

(10) Frisch, M. J.; Trucks, G. W.; Schlegel, H. B.; Scuseria, G. E.; Robb, M. A.; Cheeseman, J. R.; Montgomery, J. A., Jr.; Vreven, T.; Kudin, K. N.; Burant, J. C.; Millam, J. M.; Iyengar, S. S.; Tomasi, J.; Barone, V.; Mennucci, B.; Cossi, M.; Scalmani, G.; Rega, N.; Petersson, G. A.; Nakatsuji, H.; Hada, M.; Ehara, M.; Toyota, K.; Fukuda, R.; Hasegawa, J.; Ishida, M.; Nakajima, T.; Honda, Y.; Kitao, O.; Nakai, H.; Klene, M.; Li, X.; Knox, J. E.; Hratchian, H. P.; Cross, J. B.; Bakken, V.; Adamo, C.; Jaramillo, J.; Gomperts, R.; Stratmann, R. E.; Yazyev, O.; Austin,A. J.; Cammi, R.; Pomelli, C.; Ochterski, J. W.; Ayala, P. Y.; Morokuma, K.; Voth, G. A.; Salvador, P.; Dannenberg, J. J.; Zakrzewski, V. G.; Dapprich, S.; Daniels, A. D.; Strain, M. C.; Farkas, O.; Malick, D. K.; Rabuck, A. D.; Raghavachari, K.; Foresman, J. B.; Ortiz, J. V.; Cui, Q.; Baboul, A. G.; Clifford, S.; Cioslowski, J.; Stefanov, B. B.; Liu, G.; Liashenko, A.; Piskorz, P.; Komaromi, I.; Martin, R. L.; Fox, D. J.; Keith, T.; Al-Laham, M. A.; Peng, C. Y.; Nanayakkara, A.; Challacombe, M.; Gill, P. M. W.; Johnson, B.; Chen, W.; Wong, M. W.; Gonzalez, C.; Poplez, J. A. *Gaussian 03*, Revision D.01; Gaussian, Inc.: Wallingford, CT, 2004.

(11) As shown in Scheme 1, the H−C(Me$_2$)−C9−CHO dihedral angles of the lower (TS-1) and higher (TS-2) energy transition states are 0° and 121°, respectively.

(12) For instance, the O−C−C9−CHMe$_2$ dihedral angle of **3** is 21° in the computed and 25° in the X-ray structure (Figure 4).

(13) In both **2** and **3** the same barriers were obtained when monitoring the aromatic signals, as in the case of the aldehyde **1**.

(14) Bonini, B. F.; Grossi, L.; Lunazzi, L.; Macciantelli, D. *J. Org. Chem.* **1986**, *51*, 517–522.

(15) A few examples: In the case 1-acyl,8-phenylnaphthalene derivatives the MeCO rotation barrier is 9.5 kcal mol^{-1} and that of Bu^{t}CO is 13.2 kcal mol^{-1}. Lunazzi, L.; Mazzanti, A.; Muñoz Alvarez, A. *J. Org. Chem.* **2000**, *65*, 3200–3206. In the case of 1,4-diacyl naphthalene derivatives the two barriers are 10.2 and 22.1 kcal mol^{-1}, respectively. Casarini, D.; Lunazzi, L.; Mazzanti, A.; Foresti, E. *J. Org. Chem.* **1998**, *63*, 4991–4995. And in the case of acylmesitylene derivatives the barriers are 6.1 and 19.2 kcal mol^{-1}, respectively. Casarini, D.; Lunazzi, L.; Verbeek, R. *Tetrahedron* **1996**, *52*, 2471–2480.

(16) Whereas the rotation of the MeCO group in **2** has a quite low DFT calculated barrier (3.9 kcal mol^{-1}), that for the complete rotation of the Bu^{t}CO is computed to be much higher (15.5 kcal mol^{-1}), as expected according to ref 15. The effect of this motion (see also Figure S-5 in the Supporting Information) is, however, NMR invisible in **3** because, when such a rotation is frozen, the molecule adopts solely the preferred conformation shown in Figure 4. In this situation the small amplitude libration of 21° [12]about the plane defined by the dihedral O−C−C9−CHMe$_2$ = 0 can still take place. This process appears to be driven by the C9−Pr^i rotation and when this combined motion is fast, it still allows the existence of a dynamic plane of symmetry, which keeps isochronous the isopropyl methyl and aromatic signals of **3**. Only when this lower energy process is also frozen will anisochronous signals be NMR detectable (the DFT computed barrier for this process is 8.0 kcal mol^{-1}, as in Table 1).

(17) This is further confirmed by the unusual high field shift observed for the acetyl methyl signal of **2** (1.53 ppm) and for the *tert*-butyl methyl signal of **3** (0.64 ppm). These groups, in fact, experience the well-known effect of the aromatic ring currents because they lay above the fluorenyl ring; see: Jackman, L. M.; Sternhell, S. *Applications of NMR Spectroscopy in Organic Chemistry*, 2nd ed.; Pergamon Press: Oxford, UK, 1969; p 95. Jennings, W. B.; Farrell, B. M.; Malone, J. F. *Acc. Chem. Res.* **2001**, *34*, 885–894. Wüthrich, K. *Angew. Chem., Int. Ed.* **2003**, *42*, 3340–3363.

1-(9-Isopropyl-9*H*-fluoren-9-yl)-ethanone (2) and 1-(9-Isopropyl-9*H*-fluoren-9-yl)-2,2-dimethylpropan-1-one (3). A solution of Me-Li (2 mL, 3 mmol, 1.5 M solution in Et_2O) was added dropwise to a stirred solution of 9-isopropyl-9*H*-fluorene-9-carbaldehyde (0.47 g, 2 mmol in 20 mL of dry THF), kept at −78 °C under nitrogen. After the addition, the mixture was stirred at −78 °C for about 2 h, then CH_3OH (5 mL) was added at −78 °C. The solution was allowed to warm to room temperature, and quenched with aqueous NH_4Cl. After extraction with Et_2O, the organic layer was dried (Na_2SO_4) and the solvent was removed at reduced pressure. The crude was identified by GCMS to contain mainly the intermediate alcohol. Oxidation was carried on at room temperature by adding H_2SO_4 (0.2 mL, 1 N solution) and aliquots of CrO_3 to an acetone solution of the crude alcohol,[18]following the reaction by GC-MS. When the alcohol disappeared, acetone was removed at reduced pressure, than H_2O and Et_2O were added. The organic layer was separated and dried (Na_2SO_4), and the solvent was removed at reduced pressure. The crude was purified on a silica gel column (hexanes/acetone 9:1) to obtain a fraction containing the title compound and 9-isopropyl-9*H*-fluorene. Analytically pure samples of **2** were obtained by semipreparative HPLC (C18 column, 250 × 21.2, acetonitrile/H_2O 80:20 v/v). The same methodology was employed in the preparation of **3**, using *t*-Bu-Li (1.5 M in pentane). Analytically pure samples of **3** were obtained by semipreparative HPLC (C18 column, 250 × 21.2, acetonitrile/H_2O 90:10 v/v). Crystals of **3**, suitable for X-ray diffraction, were obtained by slow evaporation of the acetonitrile from a 1:1 solution of acetonitrile/H_2O.

1-(9-Isopropyl-9*H*-fluoren-9-yl)-ethanone (2). ^{1}H NMR (600 MHz, CD_3CN, +25 °C) δ 0.66 (d, J = 6.9H, 6H), 1.53 (s, 3H), 3.03 (septet, J = 6.9 Hz, 1H), 7.37 (td, J = 7.5, 1.2 Hz, 2H), 7.47−7.50 (m, 4H), 7.89 (m, 2H). ^{13}C NMR (150.8 MHz, CD_3CN, +25 °C) δ 18.9 (CH_3), 28.1 (CH_3), 34.38 (CH), 74.1 (C_q), 121.6 (CH), 126.5 (CH), 129.0 (CH), 129.7 (CH), 143.5 (C_q), 146.0 (C_q), 208.4 (CO). MS *m*/*z* (%) 250 ($M^{\bullet+}$, 59), 207 (100), 192 (89), 191 (72), 165 (67). HRMS calcd for $C_{18}H_{18}O$ 250.13576, found 250.1357.

1-(9-Isopropyl-9*H*-fluoren-9-yl)-2,2-dimethylpropan-1-one (3). ^{1}H NMR (600 MHz, CD_3CN, +25 °C) δ 0.53 (d, J = 6.9 Hz, 6H), 0.64 (s, 9H), 3.02 (septet, J = 6.9 Hz, 1H), 7.36 (td, J = 7.4, 1.2 Hz, 2H), 7.40 (d, J = 7.7, 2H), 7.48 (td, J = 7.4, 1.2 Hz, 2H), 7.87 (d, J = 7.6, 2H). ^{13}C NMR (150.8 MHz, CD_3CN, +25 °C) δ 18.6 (CH_3), 28.4 (CH_3), 36.0 (CH), 47.6 (C_q), 73.7 (C_q), 121.6 (CH), 126.6 (CH), 128.6 (CH), 129.5 (CH), 144.0 (C_q), 146.0 (C_q), 214.1 (CO). MS *m*/*z* (%) 292 ($M^{\bullet+}$, 4), 208 (21), 207 (100), 192 (65), 191 (28), 165 (29), 85 (31), 57(91). HRMS calcd for $C_{21}H_{24}O$ 292.18272, found 292.1826.

(18) Muller, P.; Blanc, J. *Helv. Chim. Acta* **1979**, *62*, 1980–1984.

NMR Spectroscopy. The spectra were recorded at 600 MHz for ^{1}H and 150.8 MHz for ^{13}C. The assignments of the ^{13}C signals were obtained by means of the DEPT sequence. The samples for obtaining the very low temperature spectra were prepared by connecting to a vacuum line the NMR tubes containing the compound and a small amount of C_6D_6 (for locking purposes), and condensing therein the gaseous CHF_2Cl and $CHFCl_2$ (4:1 v/v) under cooling with liquid nitrogen. The tubes were subsequently sealed in vacuo and introduced into the precooled probe of the spectrometer. Temperature calibrations were performed before the experiments, using a Cu/Ni thermocouple immersed in a dummy sample tube filled with isopentane, and under conditions as nearly identical as possible. The uncertainty in the temperatures was estimated from the calibration curve to be ±2 °C. The line shape simulations were performed by means of a PC version of the QCPE program DNMR 6 no. 633, Indiana University, Bloomington, IN.

Calculations. Geometry optimizations were carried out at the B3LYP/6-31G(d) level by means of the Gaussian 03 series of programs[10](see the Supporting Information). The standard Berny algorithm in redundant internal coordinates and default criteria of convergence were employed in all the calculations.[19]Harmonic vibrational frequencies were calculated for all the stationary points. For each optimized ground state the frequency analysis showed the absence of imaginary frequencies, whereas each transition state showed a single imaginary frequency. Visual inspection of the corresponding normal mode was used to confirm that the correct transition state had been found

Acknowledgment. L.L. and A.M. received financial support from the University of Bologna (RFO) and from MUR-COFIN 2005, Rome (national project "Stereoselection in Organic Synthesis"). D.C. received financial support from the University of Basilicata (RIL-2008).

Supporting Information Available: Variable-temperature NMR spectra of compounds **1**−**3**, MMX computed energy surface of **3**, synthetic procedure and spectroscopic data of **1**−**3** and their intermediates, X-ray data of compound **3**, ^{1}H and ^{13}C NMR spectra and HPLC traces of **1**−**3**, and computational data of **1**−**3**. This material is available free of charge via the Internet at http://pubs.acs.org.

JO8008897

(19) Thermodynamic corrections were also applied in standard conditions, using unscaled harmonic frequencies, and the corresponding results are reported in Tables S1−3 of the Supporting Information. However, these values cannot be meaningfully compared to the present experimental data because of the different temperatures, and to relevant errors in the computation of the entropic factor (see for instance: Ayala, P. Y.; Schlegel, H. B. *J. Chem. Phys.* **1998**, *108*, 2314–2325).